

Steric and Electronic Effects on the ^{103}Rh NMR Chemical Shifts of Rh^{I} (cyclooctadiene) Compounds Bearing N-Donor Ligands

Johannes G. Donkervoort,^[a] Michael Bühl,^{*[b]} Jan Meine Ernsting,^[a]
and Cornelis J. Elsevier^{*[a]}

Keywords: ^{103}Rh NMR / Rhodium complexes / Nitrogen ligands / Chemical-shift computation

In order to study electronic and steric effects on $\delta(^{103}\text{Rh})$, the ^{103}Rh -NMR spectra of a series of $[\text{Rh}(\text{cod})\text{L}_2]$ complexes (with L = nitrogen, oxygen, or chloride) have been measured by gradient-enhanced HMQC (^1H , ^{103}Rh) NMR spectroscopy. Density functional computations of representative examples have been performed at the GIAO-B3LYP level of theory. The obtained experimental values of ^{103}Rh shifts fit the generally

observed trend of coordinating ligands in the first coordination sphere of the metal: $\text{P} < \text{N} < \text{O}$. Calculated ^{103}Rh shifts agreed to within 8 % with experimental values. The computational results indicate that the Rh–N bond distance has a larger influence on the chemical shift than the N–Rh–N angle.

Introduction

Since the development of modern inverse 2D NMR techniques, a rapid growth of available NMR data concerning insensitive metal nuclei can be discerned.^[1] For example, inverse 2D X $\{^{103}\text{Rh}\}$ NMR leads to a theoretical sensitivity enhancement of 360 for X = ^{31}P and 5630 for X = ^1H , respectively. Despite the larger amount of NMR data there is still a lack of understanding of the factors which determine the chemical shift of transition metal nuclei. From the published data it has, for instance, been concluded that changes in the first coordination sphere of the Rh nucleus result in deshielding of the metal center in the order: $\text{O} > \text{Cl} \approx \text{N} > \text{Br} > \text{I} > \text{S} \approx \text{Se} > \text{Te} > \text{P} \approx \text{As} \approx \text{Sb} \approx \text{H} \approx \text{C}^* \approx \text{C}$ ($\text{C}^* = \text{sp}^2\text{-carbon}$).^[2]

It is generally accepted that the chemical shift variation of a transition metal nucleus in its coordination compound is mainly determined by the paramagnetic shielding term given by the Ramsey equation^[3] which was later developed by Griffith and Orgel (Eq. 1)^[4]. In this equation r_{d} is the expectation value of the d-orbital radius, ΣQ_{N} is the angular imbalance of charge and ΔE is the average excitation energy between the filled and empty d-orbitals.

$$\sigma_{\text{p}} = \text{const.} (\Delta E)^{-1} <r_{\text{d}}^{-3}> \Sigma Q_{\text{N}} \quad (1)$$

Changes in ΣQ_{N} generally bear a large influence on σ_{p} . Therefore this study is focused on four-coordinate, square planar Rh^{I} complexes of the general type $[\text{Rh}(\text{cod})\text{L}_2]$. In these complexes the d-electron configuration and the sym-

metry at the metal are kept constant and a discussion of the observed Rh shifts can be focused on ΔE and r_{d} alone.^[5] As earlier results indicated a dependence of the Rh shift on the applied diene,^[6] only cod complexes were used in this investigation.

We have previously studied the complexes $[\text{Rh}(\text{cod})(\text{P})_2]$ ^[6c] and observed that variations in the first coordination sphere of the Rh nucleus indeed influenced the ^{103}Rh chemical shift according to the general order given above.^[2] However, changes in the second coordination sphere, for example bite angle variations, contradicted expectations based on simple MO considerations and the Ramsey equation. This study is focussed on a series of $[\text{Rh}(\text{cod})(\text{N})_2]$ complexes in order to evaluate changes of the ^{103}Rh shift upon a systematic variation of the nitrogen ligands. These results will be discussed in the light of theoretical calculations of $\delta(^{103}\text{Rh})$ for several of the prepared complexes, which have recently become feasible.^{[7][8]} Together, these efforts may result in a better insight in the factors determining variations of the $\delta(^{103}\text{Rh})$.

Results and Discussion

Synthesis

The complexes were prepared according to literature procedures except for the new four-coordinate $[\text{Rh}(\text{cod})(\text{iPrDAB})]\text{ClO}_4$ ($\text{iPrDAB} = \text{iPrN}=\text{CH}-\text{CH}=\text{N}-\text{iPr}$), **7**. Compound **7** was obtained as a dark-green solid by adding a solution of the free ligand in acetone to a solution of in situ prepared $[\text{Rh}(\text{cod})(\text{acetone})_2]\text{ClO}_4$ in acetone (see Experimental Section). This complex is an air-stable solid with a melting or decomposition point which lies above 300 °C. Complex **7** is readily soluble in chlorinated solvents whereas it is only slightly soluble in EtOH and MeOH.

The ^1H - and ^{13}C -NMR spectra of samples of **7** in CDCl_3 or CD_3OD at ambient temperature are consistent with a

^[a] Institute of Molecular Chemistry, Universiteit van Amsterdam, Nieuwe Achtergracht 166, 1018 WV Amsterdam, The Netherlands

Fax: (internat.) +31 (0)20/ 5256456
E-mail: else4@anorg.chem.uva.nl

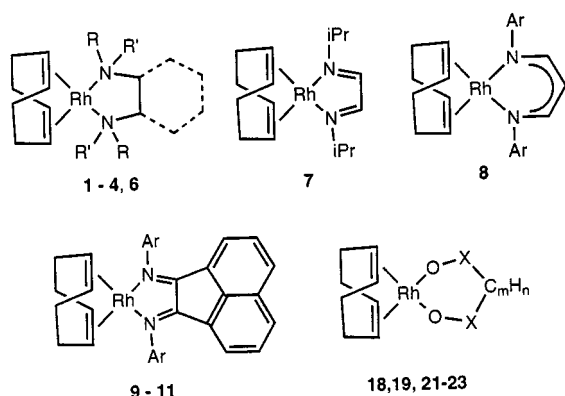
^[b] Organisch-chemisches Institut, Universität Zürich, Winterthurerstraße 192, CH-8057 Zürich, Switzerland
Fax: (internat.) +41 (0)16356836
E-mail: buehl@oci.unizh.ch

time-average C_{2v} -symmetric molecule. No dependence on the temperature has been observed by VT-NMR spectroscopy.

GE¹⁰³Rh-NMR Spectroscopy

The use of gradient selection is nowadays used for most 2D $^1\text{H}\{^{13}\text{C}\}$ and $^1\text{H}\{^{15}\text{N}\}$ experiments. Here we present the use of gradient selection to reduce the measuring time of $^1\text{H}\{^{103}\text{Rh}\}$ experiment and to reduce the ^1H signals not coupled to the rhodium more effectively. In the gradient-enhanced HMQC sequence: $^1\text{H}\text{-}^{103}\text{Rh}$ D1 – 90°(^1H) – 1/2J – 90°(^{103}Rh) – $t_1/2$ – GP1 – D16 – 180°(^1H) – GP2 – D16 – $t_1/2$ – 90°(^{103}Rh) – GP3 – 1/2J – ACQ, the equation GP1 ($\gamma\text{H} + \gamma\text{Rh}$) + GP2 ($-\gamma\text{H} + \gamma\text{Rh}$) + GP3 ($-\gamma\text{H}$) = 0 must be fulfilled. For GP1:GP2:GP3 = 90 : 44 : 50 this is true. We have tested these gradient values and compared the results with the normal HMQC pulse sequence. It was found that the number of scans per increment can be reduced from 8 or 16 to 1 or 2 without loss of information.

The ^{103}Rh NMR spectra were measured by gradient-enhanced HMQC (^1H , ^{103}Rh) as described above and in the experimental section. The compound types studied have been summarized in the drawing below and can be divided into nitrogen donor complexes (**1–15**), chloride compounds (**16, 17**) and oxygen donor complexes (**18–23**).



In order to study steric and electronic effects on the ^{103}Rh chemical shifts, density functional computations have been performed at the GIAO-B3LYP level of theory. This level has been shown to afford transition-metal chemical-shift values in good agreement with experiment for a number of organometallic compounds.^[7] In addition, it has been used to study similar steric and electronic effects on $\delta(^{103}\text{Rh})$ in related rhodium–phosphane and –cyclopentadienyl complexes.^[8] Calculations have been performed for a number of complexes of this study, comprising **1**, **2**, **5**, **6**, **7**, **13**, **14**, and **18**. The experimental ^{103}Rh chemical shifts have been collected in Table 1, together with calculated values of representative examples. The theoretical ^{103}Rh chemical shifts agree well with the corresponding experimental data, with a mean absolute deviation of 44 ppm (over a range of ca. 540 ppm). When the single large deviation in the case of **7**

Table 1. Observed^[a] and calculated^[b] ^{103}Rh NMR data for complexes **1–23**

no.	compound	$\delta^{103}\text{Rh}[\text{c}]$	
		observed	calculated
1	[Rh(cod)(1,2-en)]ClO ₄	751	725
2a	[Rh(cod)(dmeda)]ClO ₄ (trans)	784	781
2b	[Rh(cod)(dmeda)]ClO ₄ (cis)	822	801
3	[Rh(cod)(1,2-(NH ₂) ₂ C ₆ H ₄)]ClO ₄	801	
4	[Rh(cod)(1,8-(NH ₂) ₂ -naphthalene)]ClO ₄	804	
5	[Rh(cod)(1,3-pn)]ClO ₄	849	800
6a	[Rh(cod)(tmeda)]ClO ₄	978	942
6b	[Rh(cod)(tmeda)][Rh(cod)Cl ₂]	949 and 1065 ^[d]	
7	[Rh(cod)(<i>i</i> Pr-DAB)]ClO ₄	914	1088
8	[Rh(cod)(ABK)]	998 ^[e]	
9	[Rh(cod)(BIAN-R)]ClO ₄ (R = C ₆ H ₅)	1025 ^[e]	
10	[Rh(cod)(BIAN-R)]ClO ₄ (R = 2,6-(<i>i</i> Pr) ₂ C ₆ H ₃)	1057 ^[e]	
11	[Rh(cod)(BIAN-R)]ClO ₄ (R = 4-OMeC ₆ H ₄)	1059 ^[e]	
12	[Rh(cod)(4,4'-Me ₂ -bipy)]ClO ₄	795	
13	[Rh(cod)(bipy)]ClO ₄	816	810
14	[Rh(cod)(py) ₂]ClO ₄	1009	953
15	[Rh(cod)(C ₅ H ₄ N-NH-C ₅ H ₄ N)]ClO ₄	1035	
16	[Rh(cod)Cl] ₂	1093 ^[e]	
17	[Rh(cod)Cl] ₂ Et ₄ N	1107 ^[e]	1168
18	[Rh(cod)(acac)]	1287 ^[e]	1298 ^[f]
19	[Rh(cod)(1,2-(HO) ₂ -naphthalene)]ClO ₄	1301	
20	[Rh(cod)(Me ₂ CO) _x]ClO ₄	1350	
21	[Rh(cod)(dppmO ₂)]ClO ₄	1362	
22	[Rh(cod)(bipyO ₂)]ClO ₄	1362	
23	[Rh(cod)(dppeO ₂)]ClO ₄	1373	

1,2-en = 1,2-ethylenediamine; dmeda = 1,2-*N,N'*-dimethylethylenediamine; 1,3-pn = 1,3-propylenediamine; tmeda = *N,N,N',N'*-tetramethylethylenediamine; DAB = glyoxalbis(isopropylimine); ABK = acetylacetonato-bis(2,6-dimethylphenyl)ketimine anion; BIAN = bis(imino)acenaphthene; bipy = 2,2'-dipyridine; py = pyridine; acac = acetylacetonato anion; dppmO₂ = 1,1-bis(diphenylphosphane oxide)methane; dppeO₂ = 1,2-bis(diphenylphosphane oxide)ethane; bipyO₂ = *N,N'*-2,2'-dipyridine dioxide. –^[a] All complexes in CD₃OD at $T = 298$ K unless otherwise stated. –^[b] GIAO-B3LYP/II^l level (**17, 18**: basis II), see Computational Details in the Experimental Section; no counterions have been included in the calculations. –^[c] Relative to $\Xi = 3.16$ MHz; ± 1.0 ppm. –^[d] $T = 230$ K. –^[e] In CDCl₃. –^[f] See also ref.^[8a]

Table 2. Observed ^{103}Rh NMR data for phosphane rhodium complexes **24–30**

no.	compound	$\delta^{103}\text{Rh}[\text{c}]$
24	[Rh(cod)(Ph ₂ P(CH ₂) ₂ PPh ₂)]ClO ₄	–505 ^[a]
25	[Rh(cod)(PPh ₃) ₂]BPh ₄	–145 ^[b]
26	[Rh(cod)(PET ₃) ₂]BPh ₄	–132 ^[b]
27	[Rh(cod)(P ^{<i>n</i>} Bu ₃) ₂]BPh ₄	–94 ^[b]
28	[Rh(cod)(PPh ₃)(py)]PF ₆	415 ^[b]
29	[Rh(cod)(PPh ₃)(<i>p</i> -Me-py)]PF ₆	419 ^[b]
30	[Rh(cod)(PPh ₃)(<i>p</i> -Me ₂ N-py)]PF ₆	436 ^[b]

^[a] Ref.^[11] – ^[b] Ref.^[6c]

is excluded (see below for a more detailed discussion), the mean absolute deviation is improved to 30 ppm.

The range of observed chemical shifts extends from $\delta = 751$ to 1035 for the complexes containing nitrogen ligands and from $\delta = 1287$ to 1372 for those containing oxygen ligands, with an intermediate value for the chloro com-

pounds **16** and **17**. Variations in the first coordination sphere of the Rh center follow the above mentioned series given by Mann. As expected, oxygen ligands (**18–23**) cause the Rh center to be more deshielded when compared to nitrogen ligands, while phosphorous ligands (Table 2, **24–30**) result in a strongly shielded Rh center. In case of P-donors, the relative energies of occupied and vacant MOs at the ligand and the metal fragments allow for a more effective overlap in terms of σ -donation and π -backdonation. These interactions result in a larger ΔE splitting, which accounts for the strong low-frequency shift of the bis(phosphane) complexes.

In earlier studies problems were reported for $[\text{Rh}(\text{cod})\text{X}(\text{N})]$ (X = halogen, N = nitrogen ligand)^[6a] involving exchange processes. However, for all complexes mentioned in Table 1, except for $[\text{Rh}(\text{cod})(\text{tmeda})][\text{Rh}(\text{cod})\text{Cl}_2]$, **6b**, the ^{103}Rh spectra recorded at 298 K were clearly resolved. For **6b** no signal is observed at 298 K, whereas upon cooling to 230 K two signals were observed at $\delta = 949.0$ and 1065.3 . These observations can be explained by assuming the presence of two species, i.e. cationic $[\text{Rh}(\text{cod})(\text{tmeda})]^+$ and anionic $[\text{Rh}(\text{cod})\text{Cl}_2]^-$. Both the cationic and anionic species were also separately prepared as their perchlorate, **6a**, and tetraethylammonium, **17**, salt, respectively. Comparing the ^{103}Rh chemical shifts of **6a** and **17** with both observed signals of **6b** indicates that the signals at $\delta = 949.0$ and 1065.3 indeed correspond to the $[\text{Rh}(\text{cod})(\text{tmeda})]^+$ and $[\text{Rh}(\text{cod})\text{Cl}_2]^-$ species, respectively. The temperature dependence of the $\delta(^{103}\text{Rh})$ of 0.42 ppm K^{-1} and 0.52 ppm K^{-1} for $[\text{Rh}(\text{cod})(\text{tmeda})]^+$ and $[\text{Rh}(\text{cod})\text{Cl}_2]^-$, respectively, is consistent with values observed for related complexes.^[6a,9] Although different observations have indicated the presence of two species in solution for **6b**,^[10] this is the first real evidence for the presence of this cation-anion pair in solution.

For the complex $[\text{Rh}(\text{cod})(\text{dmeda})]\text{ClO}_4$, **2**, two resolved signals in a 5:1 ratio are observed in the ^{103}Rh spectra pointing to the presence of two rhodium species, **2a** and **2b**. This conclusion is corroborated by the observation of two not completely resolved sets of signals for the dmeda protons in the ^1H -NMR spectrum. Most probably these two signals arise from the presence of two stereoisomers with the methyl groups in trans (**2a**) or in cis positions (**2b**) (Figure 1). This conclusion is corroborated by results from density functional computations (vide infra), which would predict a 10:1 molar ratio for **2a** and **2b**, respectively, based on the relative energies (**2a** lower than **2b** by 5.4 kJ/mol at the B3LYP/II' level). In addition, the calculated chemical shifts for **2a** and **2b** are in good agreement with both observed values (see Table 1).

It has been proposed that the metal shift parallels the variation of the bulk and basicity of the ligand. In a systematic study of Rh–phosphane complexes,^[6c] it was shown that an increase in basicity of the phosphane ligands results in a more shielded Rh nucleus and hence a $\delta(^{103}\text{Rh})$ shift towards higher frequencies. In addition, a larger cone-angle of the phosphane ligand also results in a shift towards higher frequencies.

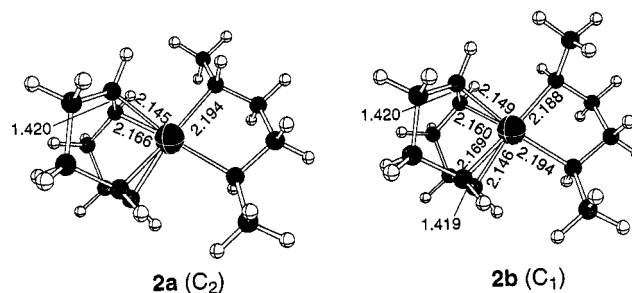


Figure 1. Optimized structures of **2a** and **2b**

For the nitrogen–rhodium complexes of this study, similar trends in the $\delta(^{103}\text{Rh})$ can be observed when looking at one class of comparable nitrogen ligands. For example, within the class of bidentate amine-ligands a high-frequency shift is observed upon increasing the Brønsted basicity of the ligand (cf. **1**, **2**, and **6**). This trend is in contrast with expectations based on simple MO considerations combined with the above mentioned Ramsey equation. A more basic ligand is expected to result in an increased ΔE which, according to the Ramsey equation, should result in a more shielded nucleus and hence a low-frequency chemical shift. The observation that simple MO considerations do not fit the Ramsey equation were also found for phosphane-rhodium complexes.^[6c]

In the series of the pyridine complexes (**12–15**), a strong chelate effect is observed. Replacing both pyridine ligands in **14** for the bidentate bipy ligand, resulting in a five-membered metallacycle (**13**), causes a significant low-frequency shift of 197 ppm. Variations in this ring-size affect $\delta(^{103}\text{Rh})$ significantly, as is evident from the high-frequency shift upon increasing the ring-size by one (cf. **13** and **15**). This same trend is also observed for the amine (cf. **1** and **5**) and diimine complexes (cf. $[\text{Rh}(\text{cod})(\text{iPrDAB})]$, **7**, $[\text{Rh}(\text{cod})(\text{ABK})]$, **8**, and $[\text{Rh}(\text{cod})(\text{BIAN-R})]$, **9–11**). The BIAN ligand systems are known to have a relatively large bite-angle due to the rigidity of the ligand back-bone, analogous to the rigidity of the 1,2-diaminobenzene ligand. Hence, the corresponding complex **3** shows a high frequency shift as compared to **1**. A similar observation has been made for some series of phosphane rhodium complexes, e.g. $[\text{Rh}(\text{nbd})(\text{Ph}_2\text{P}(\text{CH}_2)_n\text{PPh}_2)]^+$,^[11] where the experimental shift ranged from $\delta = -390$ for $n = 2$ to $\delta = -210$ for $n = 4$. Hence, the chelate-ring size appears to be one of the most important factors determining the $\delta(^{103}\text{Rh})$ value. This size effect is believed to be mediated by changes in the bite angle at the metal. Therefore, studies were performed on the model compound $[\text{Rh}(\text{cod})(\text{NH}_3)_2]^+$ by explicitly calculating its $\delta(^{103}\text{Rh})$ value as a function of the bite angle.

As apparent from the results displayed in Figure 2a, there is in fact a dependence on the bite angle of the computed $\delta(^{103}\text{Rh})$ values with a minimum near ca. 90° . Variations in the bite-angle around this 90° angle result in a more deshielded metal center and hence high-frequency shifts. Similar observations were made for rhodium(phosphane) complexes, i.e. a strong deviation from the ideal geometry of square-planar d^8 -complexes leads to a high-frequency

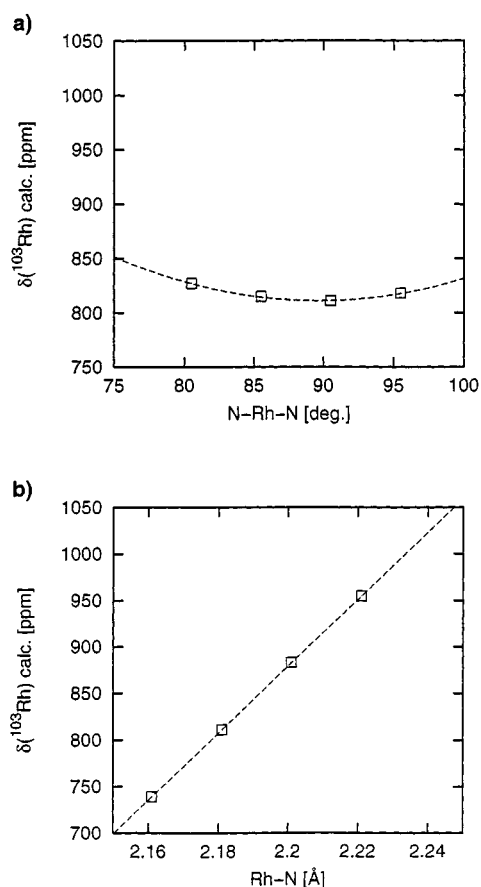


Figure 2. Calculated rhodium chemical shift of $[\text{Rh}(\text{cod})(\text{NH}_3)_2]^+$ as a function of N–Rh–N angle and Rh–N distance

shift.^{[6c][11]} However, for the model complex $[\text{Rh}(\text{cod})(\text{NH}_3)_2]^+$ there seems to be only a minor variation in $\delta(^{103}\text{Rh})$ of ca. 40 ppm in the bite-angle range between 75 and 100 typically covered in bidentate chelates. A similar result has recently been obtained in the case of rhodium(diphosphane) complexes.^[8b]

According to the latter study, the ^{103}Rh chemical shifts were found to be particularly sensitive to changes in the Rh–P bond lengths, with a computed bond-length shift derivative of more than $10,000 \text{ ppm } \text{Å}^{-1}$. The analogous study for model compound $[\text{Rh}(\text{cod})(\text{NH}_3)_2]^+$ now also revealed a large sensitivity of the computed $\delta(^{103}\text{Rh})$ value to the Rh–N bond distance (see Figure 2b), albeit with a somewhat smaller slope of $3600 \text{ ppm } \text{Å}^{-1}$. These results indicate that, although the bite-angle influences the $\delta(^{103}\text{Rh})$, mainly variations in the Rh–N bond distance dominate the $\delta(^{103}\text{Rh})$. Apparently, in rhodium–phosphane and –nitrogen complexes, variations in the chelate ring-size affect both the bite-angle and the Rh–ligand bond distance, where the latter has the larger influence on the variations in the observed $\delta(^{103}\text{Rh})$ shift.

Using these results, we tried to separate the steric and electronic effects in the series of substituted ethylenediamine complexes **1**, **2**, and **6**, the observed ^{103}Rh chemical shifts of which cover a range of 227 ppm. Contrary to expectations based on the relative Brønsted basicity of the

ligands (vide supra), a more basic ligand in this series induces a stronger deshielding of the ^{103}Rh nucleus. However, in the same series, the optimized Rh–N bond lengths increase significantly, whereas the bite angle remains essentially constant (see Table 3).^[12] According to the above-mentioned results for model compound $[\text{Rh}(\text{cod})(\text{NH}_3)_2]^+$, it is the bond-length elongation that could be responsible for the observed deshielding.

Table 3. Selected geometrical parameters of Rh(cod) complexes containing ethylenediamine derivatives and the computed $d(^{103}\text{Rh})$ chemical shifts

no.	ligand	Rh–N [Å]	N–Rh–N [°]	$\delta(\text{with Me})^{\text{[a]}}$	$\delta(\text{without Me})^{\text{[b]}}$
1	(1,2)-en	2.167	80.6	725	725
2a	dmeda (trans)	2.194	81.1	781	821
2b	dmeda (cis)	2.188/ 2.194	81.5	801	834
6	tmeda	2.239	82.2	942	974

^[a] $\delta(^{103}\text{Rh})$ computed for the fully optimized structure. ^[b] $\delta(^{103}\text{Rh})$ computed for optimized structures of the respective complexes, with Me groups substituted by H atoms.

In order to assess also the effects of the added Me groups, model calculations have been performed for the parent **1** employing the geometrical parameters optimized for the derivatives **2** and **6** (i.e. by simply replacing the Me groups with H atoms). The chemical shifts computed accordingly (last column in Table 3) are thus solely the result of the structural distortions induced by the Me groups which reflect their “pure geometrical effects”. Apparently, these distortions cause a strong deshielding, which is partly reduced by the “pure electronic effects” of the Me groups. The latter amounts to only ca. 30 ppm, as assessed by the difference between the entries of the last two columns in Table 3^[13], compared to the overall effect of up to 227 ppm observed in going from **1** to **6**. The main origin of this deshielding is therefore a geometrical, rather than an electronic effect. A comparable shielding effect (21 ppm) is observed upon substituting bipy for 4,4'-Me₂bipy, cf. the $\delta(^{103}\text{Rh})$ of **13** and **12**, respectively.

For more quantitative estimates of these geometrical effects, the bond-length shift derivative calculated for model compound $[\text{Rh}(\text{cod})(\text{NH}_3)_2]^+$, $3600 \text{ ppm } \text{Å}^{-1}$, was applied to **1**, **2**, and **6**. In going from **1** to **2** and from **1** to **6**, the optimized bond-length elongations are 0.026 and 0.072 Å, respectively. This corresponds to deshieldings of 94 and 259 ppm, respectively, which are in excellent accord with the calculated “pure geometrical effects” of 103 and 249 ppm, respectively.

For an interpretation of the steric and electronic influences, the above-mentioned influences have been discussed in terms of the parameters ΔE and r_d in the Ramsey equation. In general, it is possible to relate large differences in the first coordination sphere to the Ramsey equation by using a simplified MO theory, i.e. hard donor atoms result in more deshielded metal centers and hence in high-frequency shifts as compared to soft donor atoms (cf. rhodium complexes containing either oxygen (av. $\delta = 1300$) or phos-

phorus (av. $\delta = -100$) ligating atoms, respectively). However, trends in $\delta(^{103}\text{Rh})$ induced by second sphere variations of the applied ligands can not be related to such simplified model theories (vide supra).^[6c] A more thorough investigation into the orbital symmetry and energies of the Rh complexes seems necessary. Therefore the calculated (B3LYP) molecular orbitals of complexes **1**, **2**, **6**, **13**, **14**, and model complex $[\text{Rh}(\text{cod})(\text{NH}_3)_2]^+$ were analyzed in detail, in order to see if simple relations between appropriate ΔE values and chemical shifts could be found.

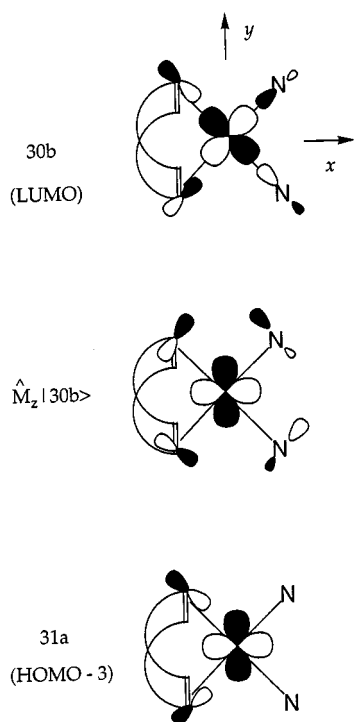


Figure 3. Highest occupied and lowest unoccupied molecular orbitals of $[\text{Rh}(\text{cod})(\text{NH}_3)_2]^+$ fragments

The four highest occupied MOs of model complex $[\text{Rh}(\text{cod})(\text{NH}_3)_2]^+$ are of predominant d(Rh) character, as expected, with some minor additional ligand contributions. At least one of the lowest unoccupied MOs also has large d(Rh) character [usually the LUMO, except when p-ligands are present such as in **13** and **14**; in these cases the LUMO is usually of $\pi^*(\text{ligand})$ character]. Magnetically induced coupling between suitable occupied and virtual MOs can account for paramagnetic contributions in a pictorial fashion. For example, in model compound $[\text{Rh}(\text{cod})(\text{NH}_3)_2]^+$ the large deshielding perpendicular to the coordination plane (z direction in Figure 3) is consistent with the coupling of the LUMO (after action of the magnetic operator \hat{M}_z on it, viz. the resulting orbital $\hat{M}_z|30b\rangle$) with an occupied MO of suitable symmetry (orbital 31a, see Figure 3).^[14] Unfortunately, it was not possible for the set of compounds under scrutiny, to simply relate the energy differences between the corresponding orbitals with the trends in $\delta(^{103}\text{Rh})$. Apparently, the particular magnetic shieldings are determined by several such interactions and it is difficult to identify a single factor, such as one particular ΔE value, as the main source for the observed trends.

The same holds for complex **7** with the *i*Pr-DAB ligand where an additional deshielding is apparent in the coordination plane (corresponding to the y axis in Figure 3), consistent with paramagnetic contributions due to the coupling of the LUMO [44b, $\pi^*(\text{DAB})$ with some $d_{xz}(\text{Rh})$ character]^[15] and the HOMO [48a, $d_{zz}(\text{Rh})$]. This is even more pronounced in the parent model compound, $[\text{Rh}(\text{cod})(\text{H-DAB})]^+$ (H-DAB = $\text{HN}=\text{CH}-\text{CH}=\text{NH}$), resulting in a huge predicted deshielding for the metal ($\delta_{\text{iso}} = 1505$). There is thus a huge shielding effect on $\delta(^{103}\text{Rh})$ upon changing the substituents at the DAB nitrogen atom from H to *i*Pr ($\Delta\delta_{\text{calc.}} = -417$ ppm). Part of this effect is due to geometrical differences, but here it is the “pure electronic effect” of the *i*Pr groups which is dominating, $\Delta\delta = -262$ ppm (assessed similarly as described above for the 1,2-en derivatives). In the DAB complexes, the ^{103}Rh chemical shift is quite sensitive to subtle changes in the electronic structure, which may be one of the reasons for the unusually large deviation (more than 170 ppm) between the theoretical and experimental $\delta(^{103}\text{Rh})$ data for **7** (see Table 1).

Conclusion

It has been found that the experimental values of the ^{103}Rh -NMR shifts of $[\text{Rh}(\text{cod})(\text{N})_2]^+$ complexes fit the expected trend according to the position within the spectrochemical series for substituents in the first coordination sphere of rhodium. Except for a diazabutadiene complex which turned out to be a problem case for theory, density-functional calculations have resulted in excellent numerical reproduction of the experimental shifts within 30 ppm, where the gross variation of shifts amounts to 540 ppm.

According to model calculations, it is the Rh–N distance that has a decisive influence upon the Rh chemical shift, rather than the N–Rh–N angle hitherto believed to be of prime importance for chelating ligands. These findings are consistent with recent results obtained for Rh–bis(phosphane) complexes. Effects of substituents in the second coordination sphere (e.g. alkyl vs. H substituents at the coordinating nitrogen atoms) can be partitioned computationally into geometrical and electronic contributions, the relative importance of which is depending on the ligand. Further interpretation of the origin of these secondary substituent effects on the metal shielding, e.g. in terms of the Ramsey equation, is difficult because it is hard to identify single, dominant parameters.

Experimental Section

NMR Techniques: Routine ^1H -NMR spectra to check purity were recorded on a Bruker AMX 300 spectrometer (300.13 MHz). All ^{103}Rh NMR measurements were carried out on a 300-MHz Bruker DRX Advance spectrometer under temperature control at 298 K using a 5-mm triple-resonance inverse probehead (^1H , $^{31}\text{P}\{\text{BB}\}$) with a z gradient coil ($90^\circ\ ^1\text{H} = 7.2$ ms, $90^\circ\ ^{103}\text{Rh} = 19.5$ ms) using the following sequence: ^1H - ^{103}Rh GS–HMQC:^[16–18] D1 – $90^\circ(^1\text{H})$ – $1/2J$ – $90^\circ(^{103}\text{Rh})$ – $t_1/2$ – GP1 – D16 – $180^\circ(^1\text{H})$ – GP2 – D16 – $t_1/2$ – $90^\circ(^{103}\text{Rh})$ – GP3 – $1/2J$ – ACQ; acqui-

sition parameters: $D1 = 1$ s, $1/J2 = 0.2-0.5$ s, $D16 = 50$ ms, $GP = 1$ ms, 1 to 4 scans were acquired per t_1 increment, block size 2048×128 points for the first experiment and 2048×256 points for the final experiment, gradient amplitudes $GP1:GP2:GP3 = 90:44:50$ G·cm⁻¹. Acquisition time 10–30 minutes for the final experiment.

The spectral width was 3000 Hz for ¹H. In the first measurement, the spectral width for ¹⁰³Rh was 9000 ppm which was covered by 128 t_1 increments, 16 dummy scans were used. To exclude folding and improve resolution, a second and sometimes third measurement with modified $n_0(\text{Rh})$ values and smaller spectral widths (at most 1900 Hz in F_1 using 256 increments) were carried out. The digital resolution of $\delta(^{103}\text{Rh})$ was at least 3.7 Hz pt⁻¹. After zero-filling in F_1 , the 512×512 matrix was transformed applying a sinebell weighing function. The ¹⁰³Rh spectrum is obtained in F_1 , and the ¹H spectrum in F_2 . The absolute ¹⁰³Rh frequency was determined by relating it to the reference frequency $\Xi = 3.16$ MHz, scaled for the operating field (¹H 9 483 491 Hz) to $\nu_{\text{ref}} = 3.16415$ MHz. Signals at higher frequencies are taken as positive.

Synthesis: All complexes, except for **7** were prepared according to published procedures: **1–3**, **5–6a**, **7**, **12–14**, **20**,^[19] **4**,^[20] **6b**,^[10] **8**,^[21] **9–11**,^[22] **15**,^[23] **16**,^[24] **17**,^[10b] **18**,^[25] **19**,^[20] **21–23**.^[26]

Preparation of [Rh(cod)(*i*Pr-DAB)]ClO₄ (7**):** To a solution of 35.6 mg (0.1444 mmol) of [Rh(cod)Cl]₂ in 25 mL of acetone was added 32.5 mg (0.1444 mmol) of AgClO₄. The resulting mixture was stirred for 15 minutes after which the formed precipitate was filtered off. To the filtrate was added a solution of 20.2 mg (0.1444 mmol) of *i*Pr-DAB in 5 mL of acetone. The reaction mixture was stirred for 10 minutes after which the solvent was removed in vacuo. The resulting green solid was washed with pentane (2 × 10 mL) and Et₂O (2 × 10 mL), respectively, and dried in vacuo. Yield 60.9 mg (0.1350 mmol) 93%. Elem. anal. for C₁₆H₂₈N₂O₄Rh found (calc.): C 42.01 (42.63), H 6.28 (6.26), N 6.14 (6.21). – ¹H NMR (CDCl₃, d): 8.34 (d, ³*J* = 2.37 Hz, 2 H, N=CH), 4.40 (s br, 4 H, HC=CH), 3.32 [s, ³*J* = 6.60 Hz, 2 H, CH(CH₃)₂], 2.54 (m, 4 H, CH₂), 2.02 (m, 4 H, CH₂), 1.34 [d, ³*J* = 6.60 Hz, 12 H, CH(CH₃)₂]. ¹³C{¹H} (CDCl₃, d): 87.47 and 87.31 (cod-CH and N=CH), 54.80 [CH(CH₃)₂], 30.42 (cod-CH₂), 22.74 [CH(CH₃)₂].

Computational Details: The same methods and basis sets as in the former theoretical studies of ¹⁰³Rh chemical shifts have been employed.^[7b,8] Geometries have been fully optimized in the given symmetry at the BP86/ECP1 level, i.e. employing the gradient-corrected exchange-correlation functionals of Becke (1988)^[27] and Perdew (1986),^[28] together with a quasi-relativistic effective core potential and the corresponding [6s5p3d] valence basis set for Rh,^[29] and standard 6–31G* basis^[30] on the ligands (designated BP86/ECP1). Magnetic shielding tensors have been computed for the BP86/ECP1 geometries with the GIAO (gauge-including atomic orbitals)-DFT method,^[31] employing a fine integration grid (75 radial shells with 302 angular points per shell), Becke's three-parameter exchange DFT/Hartree-Fock hybrid functional^[32] together with the correlation functional of Lee, Yang, and Parr^[33] (denoted B3LYP), and the following basis set (denoted basis II): Rh: well-tempered [16s10p9d] basis, contracted from the 22s14p12d set^[34] and augmented with two d-shells of the well-tempered series; ligands: IGLO-basis II recommended for chemical-shift calculations,^[35] i.e. C,N,O: (9s5p)/[5s4p] augmented with one set of d-polarization functions; Cl: (11s7p)/[7s6p] augmented with two sets of d-polarization functions; H: (5s)/[3s] polarized with one set of p-functions. For the complexes with the N-donor ligands, the chemical shift computations employed basis II', i.e. the same as basis II, but with a smaller DZ (double zeta) basis^[35] on the hydrogen atoms. For cation **1**, the GIAO-B3LYP ¹⁰³Rh shieldings differed by less than

4 ppm between basis II and basis II'. Chemical shifts $\delta(^{103}\text{Rh})$ are reported relative to $\sigma(\text{standard}) = -878$ ppm, as previously evaluated from $\sigma(\text{calc})$ vs. $\delta(\text{expt})$ linear regressions.^[7b] All calculations were performed with the Gaussian 94 program.^[36]

Acknowledgments

We kindly thank Dr. P. H. M. Budzelaar, University Nijmegen, for providing us with a sample of **8**. Financial support by the Netherlands Organization for Pure Research CW-NWO under the Young Scientists Program, is gratefully acknowledged. M. B. wishes to thank Prof. W. Thiel for continuous support. Calculations were performed on a Silicon Graphics PowerChallenge (Organisch-chemisches Institut, Universität Zürich) and on IBM RS6000 workstations (C4 cluster, ETH Zürich), as well as on a NEC-SX4 (CSCS, Manno, Switzerland).

- [1] R. Benn in: P. S. Pregosin (Ed.), *Transition Metal Nuclear Magnetic resonance*, Elsevier; Amsterdam, **1991**; p.103.
- [2] B. E. Mann in: P. S. Pregosin (Ed.), *Transition Metal Nuclear Magnetic resonance*, Elsevier; Amsterdam, **1991**; p.177.
- [3] [3a] N. F. Ramsey, *Phys. Rev.* **1950**, *77*, 567. – [3b] N. F. Ramsey, *Phys. Rev.* **1950**, *78*, 699. – [3c] N. F. Ramsey, *Phys. Rev.* **1951**, *83*, 540. – [3c] N. F. Ramsey, *Phys. Rev.* **1952**, *86*, 243.
- [4] J. S. Griffith, L. E. Orgel, *Trans. Faraday Soc.* **1957**, *53*, 601.
- [5] J. Mason, *Chem. Rev.* **1987**, *87*, 1299.
- [6] [6a] R. Bonnair, D. Davoust, N. Platzler, *Org. Magn. Reson.* **1984**, *22*, 80. – [6b] J. M. Ernsting, C. J. Elsevier, W. G. de Lange, *J. Chem. Soc., Chem. Commun.* **1989**, 585. – [6c] C. J. Elsevier, B. Kowall, H. Kragten, *Inorg. Chem.* **1995**, *34*, 4836.
- [7] [7a] G. Schreckenbach, T. Ziegler, *J. Chem. Phys.* **1995**, *99*, 606. – [7b] M. Bühl, *Chem. Phys. Lett.* **1997**, *267*, 251. – [7c] Review: M. Bühl, M. Kaupp, V. G. Malkin, O. L. Malkina, *J. Comput. Chem.*, in press.
- [8] [8a] M. Bühl, *Organometallics* **1997**, *16*, 261. – [8b] W. Leitner, M. Bühl, R. Fornika, C. Six, W. Baumann, E. Dinjus, M. Kessler, C. Krüger, A. Rufinska, submitted for publication.
- [9] K. D. Gruninger, A. Schwenk, B. E. Mann, *J. Magn. Reson.* **1980**, *41*, 354.
- [10] [10a] M. A. Garralda, L. Ibarlucea, *J. Organometal. Chem.* **1986**, *311*, 225. – [10b] M. A. Garcia, M. A. Garralda, L. Ibarlucea, *Polyhedron* **1988**, *7*, 1067.
- [11] J. M. Ernsting, C. J. Elsevier, W. G. J. de Lange, K. Timmer, *Magn. Res. Chem.* **1991**, *29*, S118.
- [12] No solid-state structures for the series **1**, **2**, and **6** are published; steric effects similar to those discussed here, however, can be noted in a cationic Rh(COD) complex with *N*-(2-aminoethyl)-piperidine as ligand (E. Anzuela, M. A. Garralda, R. Hernandez, L. Ibarlucea, E. Pinilla, M. A. Monge, *Inorg. Chim. Acta*, **1991**, *185*, 211); the Rh–N bond lengths to the primary and tertiary amine N atoms, 2.107(6) and 2.176(7) Å, respectively, are shorter than the corresponding DFT data in Table 3 (cf. entries for **1** and **6**), but the difference between these distances is very similar in both cases, ca. 7 pm elongation from primary to tertiary amine.
- [13] Somewhat counterintuitively, roughly the same effect is seen for **2** and **6** upon substituting two and four Me groups, respectively.
- [14] For similar arguments see for instance:^[14a] Y. Ruiz-Morales, G. Schreckenbach, T. Ziegler, *J. Phys. Chem.* **1996**, *100*, 3359. – [14b] Y. Ruiz-Morales, G. Schreckenbach, T. Ziegler, *Organometallics* **1996**, *15*, 3920.
- [15] Similar characteristics (i.e. ligand- π^* character and contributions from the metal) have been computed for the LUMO of other DAB complexes, which is important for their UV/vis spectra, see for instance M. P. Aarnts, M. P. Wilms, K. Peelen, J. Fraanje, K. Goubitz, F. Hartl, D. J. Stufkens, E. J. Baerends, A. Vlcek, *Inorg. Chem.* **1996**, *35*, 5468.
- [16] S. Braun, H.-O. Kalinowski, S. Berger, in *100 and More Basic NMR Experiments* **1994**, 360–363.
- [17] [17a] R. E. Hurd, B. K. John, *J. Magn. Reson.* **1991**, *91*, 648–653. – [17b] J. Ruiz-Cabello, G. W. Vuister, C. T. Moonen,

- P. van Gelderen, J. S. Cohen, P. C. M. van Zijl, *J. Magn. Reson.* **1992**, *100*, 281–303.
- [18] W. Wilker, D. Leibfritz, R. Kerssebaum, W. Bermel, *Magn. Reson. Chem.* **1993**, *31*, 287–292.
- [19] [19a] C. Cocevar, G. Mestroni, A. Camus, *J. Organometal. Chem.* **1972**, *35*, 389. — [19b] R. Uson, L. A. Oro, C. Claver, M. A. Garralda, *J. Organometal. Chem.* **1976**, *105*, 365.
- [20] L. A. Oro, M. J. Fernandez, J. Modrego, J. M. Lopez, *J. Organometal. Chem.* **1985**, *287*, 409.
- [21] P. H. M. Budzelaar, R. de Gelder, A. W. Gal, *Organometallics* **1998**, *17*, 4121.
- [22] Ch. Mahabiersing, J. G. Donkervoort, C. J. Elsevier, in preparation.
- [23] L. A. Oro, M. A. Ciriano, F. Viguri, C. Foces-Foces, F. H. Cano, *Inorg. Chim. Acta* **1986**, *115*, 65.
- [24] A. van der Ent, A. L. Onderdelinden, *Inorg. Synth.* **1990**, *28*, 90.
- [25] R. Cramer, *J. Am. Chem. Soc.* **1964**, *86*, 217.
- [26] R. Uson, L. A. Oro, M. A. Ciriano, F. J. Lahoz, *J. Organometal. Chem.* **1982**, *240*, 429.
- [27] A. D. Becke, *Phys. Rev. A* **1988**, *38*, 3098.
- [28] [28a] J. P. Perdew, *Phys. Rev. B* **1986**, *33*, 8822. — [28b] J. P. Perdew, *Phys. Rev. B* **1986**, *34*, 7406.
- [29] D. Andrae, U. Häußermann, M. Dolg, H. Stoll, H. Preuß, *Theor. Chim. Acta* **1990**, *77*, 123.
- [30] W. J. Hehre, L. Radom, P. v. R. Schleyer, J. A. Pople, *Ab initio Molecular Orbital Theory*, Wiley, New York, 1986.
- [31] As implemented in Gaussian 94: J. R. Cheeseman, G. W. Trucks, T. A. Keith and M. J. Frisch, *J. Chem. Phys.* **1996**, *104*, 5497.
- [32] A. D. Becke, *J. Chem. Phys.* **1993**, *98*, 5648.
- [33] C. Lee, W. Yang, R. G. Parr, *Phys. Rev. B* **1988**, *37*, 785.
- [34] S. Huzinaga, M. Klobukowski, *J. Mol. Struct.* **1988**, *167*, 1.
- [35] W. Kutzelnigg, U. Fleischer, M. Schundler, in *NMR Basic Principles and Progress* Vol. 23, Springer-Verlag, Berlin, 1990, 165.
- [36] M. J. Frisch, G. W. Trucks, H. B. Schlegel, P. M. W. Gill, B. G. Johnson, M. A. Robb, J. R. Cheeseman, T. Keith, G. A. Petersson, J. A. Montgomery, K. Raghavachari, M. A. Al-Laham, V. G. Zakrzewski, J. V. Ortiz, J. B. Foresman, C. Y. Peng, P. Y. Ayala, W. Chen, M. W. Wong, J. L. Andres, E. S. Replogle, R. Gomperts, R. L. Martin, D. J. Fox, J. S. Binkley, D. J. De Fries, J. Baker, J. J. P. Stewart, M. Head-Gordon, C. Gonzales, J. A. Pople, Gaussian 94, Pittsburgh PA, 1995.

Received June 30, 1998
[198207]